Evolving Transcriptomic Signature of Human Pluripotent Stem Cell-Derived Retinal Pigment Epithelium Cells With Age

Grace E. Lidgerwood [1,2,3]*, Anne Senabouth[4], Casey J.A. Smith-Anttila[5], Vikkitharan Gnanasambandapillai[4], Dominik C. Kaczorowski[4], Daniela Amann-Zalcenstein[5], Erica L. Fletcher[1], Shalin H. Naik[5,6], Alex W. Hewitt [2,3,7,#], Joseph Powell [4,8,#], Alice Pébay [1,2,3,#,]*.

[1]*Department of Anatomy and Neuroscience, The University of Melbourne, Parkville, VIC 3010, Australia*

[2] *Department of Surgery, The University of Melbourne, Parkville, VIC 3010, Australia*

[3] *Centre for Eye Research Australia, Royal Victorian Eye and Ear Hospital, East Melbourne, VIC 3002, Australia*

[4] *Garvan Weizmann Centre for Cellular Genomics, Garvan Institute of Medical Research, The Kinghorn Cancer Centre, Darlinghurst, NSW 2010, Australia*

[5] *Single Cell Open Research Endeavour (SCORE), The Walter and Eliza Hall Institute of Medical Research, Parkville, VIC 3052, Australia*

[6] *Immunology Division, The Walter and Eliza Hall Institute of Medical Research, Parkville, VIC 3052, Australia*

[7] *School of Medicine, Menzies Institute for Medical Research, University of Tasmania, Hobart, TAS 7005, Australia*

[8] *University of New South Wales Cellular Genomics Futures Institute, School of Medical Sciences, University of New South Wales, Sydney, NSW 2052, Australia*

[#] Equal senior authors

*Corresponding authors: grace.lidgerwood@unimelb.edu.au (Lidgerwood GE), apebay@unimelb.edu.au (Pébay A).

Running Title *Lidgerwood et al/ Transcriptomic Profile of hPSC-derived RPE*

Total counts. Words: 9,576; Figures: 5; Tables: 0; Supplementary Figures: 2; Supplementary Tables: 5

Abstract

We differentiated the human embryonic stem cell line H9 into retinal pigment epithelium (RPE) cells to assess temporal changes in transcriptomic profiles of cells. We performed single cell RNA-Sequencing of a total of 16,576 cells, and analysed the resulting data to access the molecular changes of RPE cells across two culture time points (1 and 12 months). Our results indicate the stability of the RPE transcriptomic signature over time in culture, with results indicating maturing populations of RPE could be observed over time, with no evidence of an epithelial – mesenchymal transition. Assessment of gene ontology (GO) pathways reveals that as cell cultures age, RPE cells upregulate expression of genes involved in metal binding and antioxidant functions, which might reflect an increased ability to handle oxidative stress as cells mature. Comparison with the transcriptional profiles of native RPE identified a progression towards a maturing RPE profile. These results suggest that *in vitro* long-term culture of RPE cells allow the modelling of phenotypes observed in native mature tissue. Our work highlights the changing transcriptional landscape of hPSC-derived RPE as they age in culture, which provides a reference for native and patient- samples to be benchmarked against.

KEYWORDS: Human Embryonic Stem Cells; Human Pluripotent Stem Cells; Retinal Pigment Epithelium; Single Cell RNA Sequencing; Aging.

Acknowledgments

This work was supported by a National Health and Medical Research Council (NHMRC) Practitioner Fellowship (AWH), Career Development Fellowship (JEP) and Senior Research Fellowship (AP, 1154389), an Australian Research Council Future Fellowship (AP, FT140100047), a NHMRC project grants (1138253 to ELF and AP; 1062820 to SHN, 1124812 to SHN), grants from the Macular Disease Foundation of Australia (AP, JEP, AWH), the Jack Brockhoff Foundation (GEL), the Ophthalmic Research Institute of Australia (AP, AWH), Stem Cells Australia – the Australian Research Council Special Research Initiative in Stem Cell Science (SHN, AWH, JEP, AP), the Mutual Trust Foundation (AP, GEL), a donation from Ms Jacqueline Pascual, the University of Melbourne and Operational Infrastructure Support from the Victorian Government.

Introduction

The retinal pigment epithelium (RPE) is a polarized monolayer of post-mitotic, pigmented cells that is essential to the health and function of photoreceptors and functionality of the underlying vasculature. The RPE phagocytoses and recycles photoreceptor outer segments – a waste product of visual cycling - and protects the retina against photo-oxidation by effectively absorbing light. It governs the exchange of fluid, nutrients, and waste products to and from the apical and basal surfaces. Laterally, tight junctions reinforce the cell network, and intercellular gap junctions couple neighboring cells, forming a structure of metabolically connected cells. This arrangement forms part of the outer blood retina barrier, a physical barrier that efficiently isolates the neural retina from systemic circulation in the underlying vascular choriocapillaris. Importantly, the RPE is key to the immune privilege of the eye, by its physical contribution to the blood retina barrier, and also its expression of molecules repressing immune cells from migrating within the retina (1).

In the human retina, aging is associated with vision decline and delayed dark adaptation, both of which are direct consequences of tissue stress and retinal damage (2). It is hypothesized that overtime, oxidative stress leads to the death of retinal neurons; a decrease in RPE numbers; an accumulation of the toxic waste lipofuscin within the RPE; and an accumulation of basal toxic deposits called drusen underneath the RPE (2). Together, these events contribute to a loss of homeostasis and low-grade inflammation within the retina (2). Although it is clear that the RPE is key to the health of the retina, the precise molecular mechanisms responsible for its aging are not well understood. We need to better understand the causal pathways behind aging – and we can only do so if we move past current methodological impasse, which highlights the fact that we cannot collect samples from living individuals, particularly from tissue such as the eye.

Human pluripotent stem cells (hPSCs), including human embryonic stem cells (hESCs) and induced pluripotent stem cells (iPSCs), have generated great expectations in the field of regenerative medicine due to their ability to propagate indefinitely *in vitro* and give rise to any cell type in the body, including cells that form the retina. A variety of protocols have been described to differentiate hPSCs into RPE cells (3–10). RPE cells are generally assayed after a few weeks of differentiation, at which stage they demonstrate similarity to their human native counterparts, in terms of morphology/expression of key proteins, functions and expression profiles, however with a profile closer to a foetal stage than adult stage (4,11,12). Interestingly, the transcriptome profile of hPSC-derived RPE cells as they age in culture is unknown. To date, the majority of RNA-seq studies have been conducted on bulk samples, consisting of millions of individual cells - the result of which is that transcript quantification represents the average signal across the cell population being studied. Recent developments to isolate single cells and genetically barcode their expressed transcripts has enabled the transcriptomes of single cells to be sequenced in a high throughput manner. By sequencing a large number of cells, it is now possible to dissect the cellular composition of apparently homogeneous cell cultures, providing a powerful way to identify and dissect molecular pathways involved in cellular events of interest. Here, we performed single cell RNA-sequencing (scRNA-seq) on hESC-derived RPE cells differentiated for 1 and 12 months to assess the impact of time in culture on the RPE transcriptome and whether genetic hallmarks of maturation can be observed overtime.

Results

Quality control

The H9 hESC line was differentiated to RPE following the protocol described in the methods section. RPE cells originating from the same cell culture of origin and the same original passaging of RPE cells were isolated after 1 and 12 months of differentiation, dissociated to single cells and processed to generate libraries for scRNA-Seq analysis, in order to generate a transcriptional map of the aging RPE cells (**Figure 1A**). The capture of the 1-month single cell library detected 12,873 cells at the mean read depth of 40,499 reads per cell, while the 12-month capture detected 4,850 cells at the mean read depth of 114,503 reads per cell (**Supplementary Table 1**). To account for the disparities between the sequencing depth of the samples, the 12-month library was down-sampled to the mean read depth of the 1-month sample. Both datasets underwent filtering where 510 cells and 637 cells were removed from the 1-month and 12-month datasets respectively, based on the distribution of the following cell-specific metrics: total number of Unique Molecular Identifiers (UMIs), number of detected genes and proportion of mitochondrial and ribosomal-related genes to total expression (**Supplementary Figure 1A-D**, **Supplementary Table 1**). The remaining 16,576 cells were retained for further analysis.

Identification and characterisation of subpopulations

Cluster analysis was performed independently and identified 12 subpopulations in each sample (**Supplementary Table 2**). After the data were integrated using anchors identified using a method described by (16), MetaNeighbor was used to match common subpopulations across both samples (17), denoted as “Common”. Clusters unique to 1-month and 12-month samples were respectively denoted as “Young” and “Aged”. In total, 18 subpopulations were identified with six common subpopulations (“Common”, 8,484 cells), six subpopulations exclusive to the 1-month dataset (“Young”, 5,758 cells) and six subpopulations exclusive to the 12-month dataset

("Aged", 2,334 cells). Conserved cluster markers for each distinct cluster (**Supplementary Tables 3-5**) and cell counts per cluster (**Figure 1B**) were identified, and clusters visualised by Uniform Manifold Approximation and Projection (UMAP) plot (**Figure 1C**). 3,070 cells could not be assigned to a subpopulation. We compared variations in the transcriptomic profiles between the 1-month-old and 12-month-old samples as to identify potential changes in phenotypes upon aging of RPE cells *in vitro*. Cell type specific markers were identified using the Find Conserved Markers function for each cluster and Gene Ontology (GO) analysis (13,14) was performed using a PANTHER overrepresentation test against the *Homo sapien* genome (PANTHER version 14.1 Released 2019-03-12). Differential expression (DE) analysis was performed using the FindMarkers function based on the Likelihood Ratio Test adapted for single cell gene expression (15). Canonical markers, gene expression profiles and their associated GO analysis specific to each cluster are provided in **Supplementary Tables 3-5.** Some clusters had insufficient gene markers for GO analysis (Aged Clusters 0, 1 and 5). We assessed the expression profile of canonical RPE genes across all subpopulations, both in terms of frequency and intensity of expression (**Figure 1D, Supplementary Tables 3-5**). Those included genes linked to extracellular structure organization (*CST3* [Cystatin C], *EFEMP1* [EGF Containing Fibulin Extracellular Matrix Protein 1], *ITGAV* [Integrin Subunit Alpha V], *CRISPLD1* [Cysteine Rich Secretory Protein LCCL Domain Containing 1], *ITGB8* [Integrin Subunit Beta 8]); tight junctions (*TJP1/ZO1* [Tight Junction Protein 1/ Zona Occludens 1]; phagocytic activity (*GULP1* [GULP PTB Domain Containing Engulfment Adaptor 1]); secretion (*SERPINF1/PEDF* [Serpin Family F Member 1/Pigment epithelium-derived factor], *VEGFA* [Vascular Endothelial Growth Factor A], *ENPP2* [Ectonucleotide Pyrophosphatase/Phosphodiesterase 2]); melanin biosynthesis (*PMEL* [premelanosome protein], *TTR* [Transthyretin], *TYR/TYRP2* [tyrosinase],

TYRP1 [tyrosinase-related protein 1], *DCT* [dopachrome tautomerase]); visual cycle (*RPE65* [Retinal pigment epithelium-specific 65 kDa protein], *LRAT* [Lecithin Retinol Acyltransferase], *BEST1* [Bestrophin 1], *RLBP1* [*CRALBP*, Retinaldehyde Binding Protein 1], *PLTP* [Phospholipid Transfer Protein], *RBP1/CRBP1* [Retinol Binding Protein 1], *RGR* [Retinal G Protein Coupled Receptor]); lipid biosynthesis (*HACD3* [3-Hydroxyacyl-CoA Dehydratase 3], *PLAAT3*/*PLA2G16* [Phospholipase A And Acyltransferase 3], *PLCE1* [Phospholipase C Epsilon 1], *PTGDS* [Prostaglandin D2 Synthase], *CYP27A1* [Cytochrome P450 Family 27 Subfamily A Member 1] and *INPP5K* [Inositol Polyphosphate-5-Phosphatase K]). Most canonical RPE genes were expressed across most populations, confirming the purity of the RPE cell cultures over time (**Figure 1D**). As these transcripts are associated with stages of RPE maturity, our data suggests that all subpopulations are of RPE lineage, potentially at various stages of differentiation and maturation. Differential gene expression analysis and pathway enrichment were performed to characterise the molecular signature of these subpopulations.

Assessment of the Common Subpopulation

Of the cells examined, more than half (8,484 cells) were clustered into "Common" subpopulations (1-6) that intersect the 1-month-old and 12-month-old cell cultures **(Figures 2-5)**, indicating a large shared transcriptional profile between the two conditions. A range of RPE markers were observed as conserved between conditions (1-month-old and 12-month-old) (**Figures 2, 3A**). In particular, RPE markers associated with melanin biosynthesis (*MITF* [Microphthalmia-associated transcription factor], *PMEL*, *TTR*, *TYR*, *TYRP1*, *DCT*), extracellular structure organization (*EFEMP1*, *CST3*, *CRISPLD1*, *ITGAV*, *ITGB8*), secretion (*SERPINF1*, *VEGFA*), visual cycle (*RPE65*, *BEST1*, *RBP1*, *RLBP1*, *PLTP*, *RGR*, *LRAT*), tight junctions

(*TJP1*), phagocytic activity (*GULP1*) and lipid biosynthesis (*PTGDS*, *CYP27A1*, *INPP5K*, *PLA2G16*, *PLCE1*) were conserved in all or in some of the various subpopulations (**Supplementary Table 3**). Examples of genes characteristics of neural differentiation, extracellular matrix and RPE are illustrated in **Figure 3B-D** respectively. Some intra-subpopulation variations in the pattern of gene expressions were observed between cells identified from the 1-month-old or 12-month-old cultures (**Figure 3B-D**).

"Common" Subpopulation One (2,282 cells) was characterised by 891 identified conserved markers (p value cut-off of <0.74) (**Supplementary Table 3**). Among the most highly conserved markers was *NDUFA4L2* (NADH dehydrogenase (ubiquinone) 1 alpha subcomplex, 4-like 2), a gene known to be associated with the macula retina (18); the zinc metalloenzyme gene *CA9* (carbonic anhydrase 9); genes involved in pigment/melanin biosynthesis such as *DCT*, *PMEL*, *MITF*, and *TYR* and *TYRP1*. This subpopulation also expresses genes involved in early retinal development including of the RPE and eye morphogenesis (*SOX4*, *EFEMP1*, *BMP7*, *VIM*, *GJA1*, *PTN*). RPE signature genes involved in the retinoid cycle were also expressed including *RPE65* and *RLBP1*. In addition, 32 *RPS* (Ribosomal Protein S), 47 *RPL* (Ribosomal Protein L) as well as 11 mitochondrially-encoded genes were identified. PANTHER GO-Slim Biological Process Overrepresentation test (Fisher exact test, FDR <0.05) analysis found an overrepresentation of pathways involved in mitochondrial and ribosomal function; protein biogenesis, transport, assembly and function; ATP biosynthesis and metabolism; and response to oxidative stress. Expression of mitochondrially-encoded genes and ribosomal genes has been correlated with development and maturation (19), including of the retina (20,21). Hence, the presence of RPE markers, together with mitochondrially-encoded genes and ribosomal genes suggests this subpopulation comprises of a highly metabolically active maturing RPE phenotype.

"Common" Subpopulation Two (2,204 cells) identified 1077 conserved markers. Its 15 most conserved markers are *CST3*, *SERPINF1*, *TTR*, *RPE65*, *CRISPLD1*, *WFDC1* (WAP Four-Disulfide Core Domain 1), *SMOC2* (SPARC Related Modular Calcium Binding 2), *DCT* (downregulation), *RBP1*, *PTGDS*, *FRZB* (downregulation), *BEST1*, *LAYN* (Layilin), which are all known RPE markers. Many of the markers expressed are involved in the generation of RPE or in their maturation and homeostasis. For instance, Cystatin C (encoded by *CST3*) is abundantly produced by RPE cells (22) and its secretion diminishes with aging (23). *DCT* is expressed in the developing retina (24), is important to the production of melanin and to the RPE homeostasis (25,26) and its downregulation is associated with mature native RPE (27). We thus suggest this subpopulation is a mature functional RPE population.

"Common" Subpopulation Three (1,811 cells) identified 1,226 conserved markers. Its most conserved markers are mostly known to be expressed in the RPE (*DCT*, *TTR*, *CST3*, *AQP1* [Aquaporine-1], *FTH1* [Ferritin Heavy Chain 1] (28), *FRZB*, *BEST1*), with some markers, such as *TFPI2* (Tissue Factor Pathway Inhibitor 2), known to promote survival and maintenance of RPE cells (29). The markers are similar to those of the "Common" Subpopulation Two. Other markers identified are not necessarily RPE-specific. For instance, *GNGT1* (G Protein Subunit Gamma Transducin 1) encodes for a protein found in rod outer segments could suggest that cells are not yet fully committed. Together, those markers indicate cellular functions suggestive of functional and maturing RPE cells.

"Common" Subpopulation Four (1,170 cells) identified 1,421 conserved markers. Many of the most conserved markers of this subpopulation are not specifically linked to the RPE. For instance, *TMSB4X* (Thymosin Beta 4 X-Linked) is linked to the cytoplasmic sequestering of NF-kappaB but has not yet been associated to molecular events in RPE cells, whilst many others are

associated with the cytoskeleton, such as *TAGLN* (Transgelin, actin binding protein), *TNNC1* (Troponin C1, Slow Skeletal And Cardiac Type), *CALD1* (Caldesmon 1), *MYLK* (Myosin Light Chain Kinase), *TPM1* (Tropomyosin 1), *ACTA2* (Actin Alpha 2, Smooth Muscle), *MYL9* (Myosin Light Chain 9). On the other hand, the presence of markers known to be expressed by the RPE (including *TTR*, *BEST1*, *CST3*, *CSTV* [Cathepsin V] (30), *CRYAB*, *SERPINF1*, *PMEL*, *VEGFA*, *RBP1*, *RLBP1*, *TYR*, *TYRP1*) confirms the RPE identity of the subpopulation. The presence of genes associated with early differentiation, such as *IGFBP5* (Insulin Like Growth Factor Binding Protein 5, downregulated, as observed upon RPE differentiation (31)) and *CRB2* (Crumbs Cell Polarity Complex Component 2) (32), involved in RPE polarity (33) suggest an early stage of RPE maturity. This pattern is suggestive of a differentiating RPE population.

"Common" Subpopulation Five (630 cells; 907 conserved markers) was characterised by RPE markers being conserved (including *SERPINE2* (34), *AQP1* (downregulated relative to cells of the same condition in other clusters, referred to as "downregulated"), *CST3* (downregulated), *SFRP5* (Secreted Frizzled Related Protein 5 (35)), *LAYN*, *PTGDS* (downregulated), *SERPINEF1* (downregulated), *BEST1* (downregulated), *SMOC2* (downregulated)). Other genes indicate an immaturity/ differentiation or proliferation of cells, such as *GAP43* (Growth Associated Protein 43), *DAAM1* (Dishevelled Associated Activator Of Morphogenesis 1), *CD44* (36), *DUSP4* (Dual Specificity Phosphatase 4). Further, the downregulation of some RPE markers suggests this subpopulation comprises of early differentiation to RPE.

Finally, "Common" Subpopulation Six (387 cells; 1,664 conserved markers) was characterised by markers associated with retinal cell types other than RPE (37) (such as *SPP1* [Secreted Phosphoprotein 1/Osteopontin], *CPODXL* [Podocalyxin Like], *STAC2* (SH3 And Cysteine Rich Domain 2), *PCDH9* [Protocadherin 9]) or found at low levels in the RPE (such as

CPAMD8 [C3 And PZP Like Alpha-2-Macroglobulin Domain Containing 8] and *SFRP2 (38)*). Only the marker *CRABP1* was highly conserved and upregulated, whilst other RPE markers were downregulated (such as *SERPINF1*, *BEST1*, *RLBP1* or *RPE65*). This thus suggests a subpopulation of immature cells.

Upregulated and statistically significant ($p<0.05$) GO-Slim Biological Pathways conserved within the "Common" subpopulations were predominantly involved in mitochondrial, metabolic and ribosomal processes (**Figure 4, Supplementary Table 3)**. Purine biosynthesis, nucleotide metabolism and protein biogenesis, localisation and transport were all significantly upregulated in the analysis. Amongst the downregulated biological processes were pathways related to sensory perception, synaptic signalling, and immune responses including B cell activation, immune response and defense against bacteria (**Figure 4, Supplementary Table 3)**.

Altogether our data suggests that the common population to both time points is heterogenous, with subpopulations representing different stages of RPE cell differentiation.

Assessment of the Young Subpopulation

Around a third of all cells (5,625 cells) clustered into the "Young" subpopulation (**Supplementary Table 4**). Common RPE markers were found to be conserved markers within a few "Young" subpopulations (**Figures 2, 3A, Supplementary Table 4**). These were associated with melanin biosynthesis (*PMEL*, *TTR*, *TYR*, *TYRP1*, *DCT*), extracellular structure organization (*EFEMP1*, *CST3*, *CRISPLD1*, *ITGAV*, *ITGB8*), secretion (*SERPINF1*, *VEGFA*, *ENPP2*), visual cycle (*BEST1*, *RBP1*, *RLBP1*, *RGR*), phagocytic activity (*GULP1*) and lipid biosynthesis (*PTGDS*).

"Young" Subpopulation Zero (2,219 cells; 20 conserved markers) showed expression of *SERPINF1*, *CST3*, *DCT*, *TSC22D4* (TSC22 Domain Family Member 4), *IGFBP5* (Insulin Like Growth Factor Binding Protein 5), *RNASE1* (Ribonuclease A Family Member 1, Pancreatic). Most have been reported in the retina (Courtesy of Human Protein Atlas, www.proteinatlas.org) (37) including for some in the human RPE (*IGFBP5* (31)).

"Young" Subpopulation One (1,873 cells; 58 conserved markers) was characterised by gene expression of *CTNNB1* (Catenin Beta 1), *NOG* (Noggin) *ATP1B1* (ATPase Na^+/K^+ Transporting Subunit Beta 1), *GSTP1* (Glutathione S-Transferase Pi 1), *CD63* (CD63 Molecule), *HNRNPH1* (Heterogeneous Nuclear Ribonucleoprotein H1). All play fundamental roles for the homeostasis and functions of the RPE: *ATP1B1* encodes an apical Na^+/K^+ ATPase which expression reduces with age and in AMD (39); defects in *CTNNB1* are linked to abnormalities in RPE development and pigmentation (40); GSTP1 is a survival factor for RPE cells, which levels increase as cells mature (41); CD63 is a late endosome/exosome marker known to be released by RPE cells (42) and *HNRNPH1* levels are associated with improved survival of RPE cells in culture (43). Hence, those markers indicate cellular functions suggestive of functional RPE cells. It is interesting to note that known canonical RPE markers, such as *SERPINF1*, *RLBP1*, *TTR*, *PMEL*, *CRYAB* (Crystallin Alpha B) were less expressed in this subpopulation than in all other subpopulations. This could indicate a stage of differentiation/ maturation of the RPE cells.

"Young" Subpopulation Two (144 cells; 16 conserved markers) was characterised by the specific upregulation of genes including *CCL2* (C-C Motif Chemokine Ligand 2), *SFRP1* and *B2M* (Beta-2-Microglobulin), which are implicated in the negative regulation of epithelial cell proliferation. Downregulation of *CTSV* (Cathepsin V) and *TMSB4X* (Thymosin Beta 4 X-Linked), linked to the cytoplasmic sequestering of NF-κB but have not yet been associated to

molecular events in RPE cells together with the expression of *DCT*, known to be expressed during RPE development (44), suggests an immature RPE population.

"Young" Subpopulation Three (67 cells; 369 conserved markers) was characterised by the expression of genes such as *TOP2A* (DNA Topoisomerase II Alpha), *PCLAF* (PCNA Clamp Associated Factor), *PTTG1* (PTTG1 Regulator Of Sister Chromatid Separation, Securin), *ANLN* (Anillin Actin Binding Protein), *MKI67* (Marker Of Proliferation Ki-67), *RRM2* (Ribonucleotide Reductase Regulatory Subunit M2), *TPX2* (TPX2 Microtubule Nucleation Factor), *PBK* (PDZ Binding Kinase). Although all genes are found to be expressed in the retina (37), none are associated to a specific RPE signature. However, they are associated with cell proliferation (*TOP2A*, *PCLAF*, *PTTG1*, *MKI67*, *RRM2*, *TPX2*, *PBK)* and cellular rearrangements (*ANLN*), which have been described as characteristics of immature RPE cells (45). In particular, ANLN is reported to promote maturity of intercellular adhesions (tight junctions and adherens junctions) in epithelial cells (46). TOP2A is associated with retinal development and proliferation (47), which combined with expression of *PCLAF*, *PTTG1 and MKI67* suggests a proliferating cell population. Low expression of RPE markers (*RBP1*, *ENPP2*, *CRABP1*, *HNRNPH1*) further suggests the RPE identity of the developing retinal cell subpopulation. Altogether, this expression profile suggests an immature differentiating cell population.

Similarly, "Young" Subpopulation Four (871 cells; 49 conserved markers) was characterised by expression of genes that are not traditionally associated with the RPE identity. The expression of *CRYAB* (downregulated), *CRX*, *FTH1*, *TFPI2* (Tissue Factor Pathway Inhibitor 2, known to promote survival and maintenance of RPE cells (29)) and *DCT*, expressed in the native RPE, suggests a differentiation to RPE yet the presence of the photoreceptor specific *GNGT1* could suggest an early differentiation step where cells are not yet fully committed.

Interestingly, "Young" Subpopulation Five (584 cells; 99 conserved markers) displays a signature comprising mitochondrial and ribosomal -related transcripts. It expresses mitochondrial-related genes (*MT-CO1* [Mitochondrially Encoded Cytochrome C Oxidase I1], *MT-CO2*, *MT-CO3*, *MT-ND3* [Mitochondrially Encoded NADH:Ubiquinone Oxidoreductase Core Subunit 3], *MT-ND4*, *MT-ND5*, *MT-ATP6* [Mitochondrially Encoded ATP Synthase Membrane Subunit 6]) and ribosomal genes *RPS2* (Ribosomal Protein S2), *RPS4X* (Ribosomal Protein S4 X-Linked), *RPS6*, *RPS8*, *RPS18*, *RPS27*, *RPL1* (Ribosomal Protein L1), *RPL3*, *RPL7*, *RPL10*, *RPL15*, *RPL29*, *RPL34*, *RPL41*. These genes are ubiquitous and have not been specifically correlated to the retina or the RPE, however they are known to facilitate fundamental processes of biology, including electron transfer and energy provision, ribosome biogenesis and protein synthesis. This subpopulation also expresses RPE markers, such as *BEST1*, *VEGFA*, *ENPP2*, *TIMP3*, *TYRP1* as well as genes involved in early retinal development including of the RPE and eye morphogenesis (*SOX11*, *PMEL*, *EFEMP1*, *BMP7*, *VIM*, *GJA1*, *PTN*) (24,48). Hence the presence of high level of expression of mitochondrial-encoded genes and ribosomal-related genes in RPE are suggestive of highly active cells with high protein synthesis and of a maturing RPE population.

Taken together, our results suggest that all subpopulations within the "Young" cohort are immature cells developing to RPE cells.

Assessment of the Aged Subpopulation

Less than 10% of all cells (2,334 cells) clustered into the "Aged" subpopulation (**Supplementary Table 5**). All six identified "Aged" subpopulations were subjected to the same analysis; however, a statistical overrepresentation test returned no positive results for "Aged"

Subpopulations Zero, One and Five (most likely owing to the low number of conserved genes identified). Only a few common RPE markers associated with melanin biosynthesis (*TTR*, *DCT*), extracellular structure organization (*CST3*, *CRISPLD1*), secretion (*SERPINF1*, *VEGFA*), visual cycle (*RLBP1*) and lipid biosynthesis (*INPP5K*) were conserved in some of the "Aged" subpopulations (**Figures 2, 3A, Supplementary Table 5**).

"Aged" Subpopulation Zero (851 cells; 6 conserved markers) showcased more cells expressing *CRISPLD1*, *PCCA* (Propionyl-CoA Carboxylase Subunit Alpha), *WFDC1*, *TTR*, *SH3BGRL3* (SH3 Domain Binding Glutamate Rich Protein Like 3) and *TMSB4X* yet with lower average levels of expression per cell than those observed in all other subpopulations. Some of these genes have been found to be expressed in the RPE (*CRISPLD1*, *WFDC1* (49), *TTR*, *TMSB4X* (44) and are associated with late RPE development (*CRISPLD1*, *TTR* (24)), whilst others have a wider expression pattern (*PCCA*, *SH3BGRL3*) and encodes for proteins involved in more universal cellular events: mitochondrial protein PCCA playing roles in death/survival, SH3BGRL3 is involved in oxidoreduction, whilst *TMSB4X* encodes proteins of the cytoskeleton. A similar pattern of expression was observed in "Aged" Subpopulation One (815 cells; 12 conserved markers) showing more cells expressing *HSD17B2* (Hydroxysteroid 17-Beta Dehydrogenase 2), *TPM1, MYL9, NDUFA4L2*, *BNIP3* (BCL2 Interacting Protein 3), *CALD1*, *TTR*, *DCT*, *MT-CYB* [Mitochondrially Encoded Cytochrome B], *FTH1*, *CRYAB* and *TMSB4X* but at lower average levels per cell than in all other subpopulations. Nine out of the twelve genes are known to be expressed in the RPE (*TTR*, *TMSB4X* (44), *CALD1* (50), *DCT* (44), *HSD17B2 (51)*, *NDUFA4L2 (24)*, *BNIP3* (28), *FTH1 (28)*, *CRYAB*). Some of these markers are associated with late RPE development (*TTR* (24)) whilst others are associated with a geographic localisation of cells within the retina (*HSD17B2 (52)*, *NDUFA4L2* (18)). *BNIP3*, *NDUFA4L2*

encode for mitochondrial proteins playing roles in death/survival and electron transport, whilst *TPM1*, *MYL9*, *TMSB4X*, *CALD1* encode proteins of the cytoskeleton. A similar pattern of expression was observed with "Aged" Subpopulation Five (170 cells; 6 conserved markers) with *PCCA*, *WFDC1*, *SERPINE2*, *TMSB4X*, *TTR* being expressed in more cells with lower average levels than compared to all other subpopulations. *SPON2* (Spondin 2) was expressed in more cells and at higher levels and encodes for extracellular matrix proteins important for cell adhesion. The close similarity of these three "Aged" subpopulations suggest a late RPE phenotype, with higher levels of maturation, towards regionalisation of cells.

Similarly, "Aged" Subpopulations Two (46 cells; 22 conserved markers), Three (32 cells; 121 conserved markers) and Four (420 cells; 33 conserved markers) show close similarities in terms of gene expression profile. The presence of known RPE markers (such as *DCT* (Subpopulation Two, downregulated), *CALD1* (Subpopulation Two, downregulated), *TTR* (Subpopulation Three, downregulated; Subpopulation Four), *SOX9* (Subpopulation Three, downregulated), *RBP1* (Subpopulation Three, downregulated; Subpopulation Four), *TMSB4X* (downregulated in all three subpopulations), *CRYAB* (downregulated in Subpopulations Two and Three) confirms their RPE identity.

Results from PANTHER Overrepresentation Tests on "Aged" Subpopulations Two and Four were similar, with high significance in pathways associated with response to metal ions (particularly cadmium, copper, iron and zinc); response to stress, chemicals and toxins; and neural crest fate commitment, which was the most significantly identified biological process in the "Aged" Subpopulation Three, with a 92.9-fold enrichment. Interestingly, GO analysis indicates that genes involved in metal binding, in particular of zinc (*MT1E*, *MT1F*, *MT1G*, *MT2A*, *MT1X*), metal iron (*MT1E*, *MT1F*, *MT1G*, *DCT*, *MT2A*, *MT1X*) and copper iron (*DCT*) as

well as in oxidoreduction (*DCT*) were significantly differentially expressed between the "Aged" subpopulations compared to all others, with an overall increased expression per cell as cells age (**Supplementary Table 5)**. This data suggests that the RPE cells of these "Aged" subpopulations are increasing their handling of metals and antioxidant abilities, which could reflect a further maturation of the RPE cells.

Other genes and pathways of interest

RPE cells express many complement components in various retinal diseases, inflammation and/or aging (53). The complement regulators *C1s* (Complement C1s), *C1r* (Complement C1r) and *C1QBP* which form the C1 complex were conserved markers in a few "Young" and "Common" subpopulations (all in "Common" Subpopulation Three; *C1s* and *C1r* in "Young" Subpopulation Five and "Common" Subpopulations One and Five; *C1r* and *C1QBP* in "Common" Subpopulation Two; *C1s* "Common" Subpopulation Four; *C1r* only "Common" Subpopulations Two and Six; *C1QBP* only in "Common" Subpopulations Two, Three and Six) (**Supplementary Tables 3, 4**). Other genes associated with the complement response (such as *CFH*, *CFB*, *CFHR1*, *CFHR3*, *C3*) were not identified as markers of any subpopulation (**Supplementary Tables 3-5**). This suggests that the complement components are not modulated with time in culture.

APOE (Apolipoprotein E) plays a role in lipid metabolism, drusen content and is also modified with complement activation in the RPE (54). We observed that *APOE* is a conserved marker of the "Young" subpopulations One and Five, as well as all "Common" Subpopulations (**Supplementary Tables 3, 4**). The levels of expression per cell is however different between subpopulation, with an upregulation in the "Young" Subpopulation Five, and a downregulation

in the "Young" Subpopulation One as well as in the "Common" subpopulations One, Two, Three and Six. Interestingly, within the "Common" subpopulation Four, cells arising from the 1-month-old culture expressed less *APOE* than cells arising from 1-month culture of all other "Common" subpopulations whilst the opposite was observed with the 12-month-old cells within this subpopulation. The opposite pattern was observed in the "Common" Subpopulation Five (**Supplementary Tables 3, 4**).

Finally, it is interesting to note that no markers of EMT (such as *SNAI1*, *SNAI2*, *ZEB1*, *TWIST1*, *GSC*) were not characterised in any examined subpopulation (**Supplementary Tables 3-5**), demonstrating the stability of the cell culture over time with no evidence of a transition to a mesenchymal phenotype.

Comparison to known signatures of native RPE cells.

We compared the hPSC-derived RPE signature to that of fetal native RPE cells, which was obtained by scRNA-Seq (24). As observed foetal native tissue, the hPSC-derived RPE cells expressed *SERPINF1*, *TYR*, *MITF*, *RPE65*, *BEST1*, and *TTR*, and more immature cells expressed *SFRP2*, *MKI67* and *DCT* (**Figures 1D-3**). RPE cells expressed genes associated with secretion (*SERPINF1/PEDF*, *VEGF*), visual cycle proteins (*RPE65*, *LRAT*, *BEST1*, *TTR*, *PLTP*, *RGR*, *RLBP1*), melanin biosynthesis (*PMEL*, *TTR*, *TYRP1*, *DCT*), phagocytic activity (*MERTK*, *GULP1*), extracellular structure organization (*CST3*, *EFEMP1*, *ITGAV*, *CRISPLD1*, *ITGB8*) and lipid biosynthesis (*HACD3*, *PLA2G16*, *PLCE1*, *PTGDS*, *CYP27A1* and *INPP5K*) (**Figures 1D-3**). Some common RPE genes are expressed in the adult native RPE at much higher levels than in fetal RPE (27). Those include *RPE65*, *TTR*, *CRX*, *BEST1*, *CHRNA3*, *RBP1*, *MYRIP*, *TFPI2*, *PTGDS*, *SERPINF1*, *DUSP4* and *GEM*. Similarly, downregulation of *DCT*, *SFRP5*, *SILV*,

TYRP1, *SLC6A15* is associated with mature native RPE (27). We thus compared the expression profiles of those genes in the RPE cultures overtime, in order to assess the maturity of the cultured cells (27) (**Figure 5**). We observed that the "Common" Subpopulation (both times of culture) presented high expression of *RPE65*, *TTR*, *BEST1*, *RBP1*, *PTGDS*, *SERPINF1*, *DUSP4* and *GEM*, associated with a downregulation of *DCT* and *TYRP1* (**Supplementary Table 3**). This thus suggests that this population correlates more closely with the adult native RPE.

Discussion

Here, we provide a dynamic profile of the transcriptome of hPSC-derived RPE cells over 12 months. Our data confirms expression of markers of RPE homeostasis and functions in hESC-derived RPE (24,27,55,56) and provides novel information on the timing of expression of those markers. At both early and late time points, we observed that hPSC-derived RPE cells expressed genes associated with secretion, visual cycle, melanin synthesis, phagocytic activity, metal binding and oxidoreductase activity. Based on expression of genes known to be associated with levels of RPE maturity and on GO analysis, the identified 18 subpopulations regroup into three main populations: immature and progenitor cells, maturing RPE cells and functionally mature RPE cells. Within those, some subpopulations were comprised of highly metabolically active cells.

An essential function of the RPE is photoprotection of the retina, which is accomplished by different mechanisms. Those include absorbing radiation, binding and sequestering redox-active metals such as iron, and scavenging free radicals and reactive oxygen species (57). Metallothioneins are metal-binding proteins that are protective against oxidative stress. Compared to the 12-month-old RPE, the 1-month-old RPE cells express less mRNA for the

metallothioneins *MT1E*, *MT1F*, *MT1G*, *MT2A*, *MT1X* and higher levels of the Dopachrome Tautomerase *DCT*. This data suggests a variation in the handling of metals and in the antioxidant abilities of RPE cells, which could be reflective of either a necessity to handle more oxidative stress in an aging *in vitro* environment or a maturation of RPE cells towards a more mature and protective phenotype (57). The assessment of variations in other gene expression between the two time points indicates a maturation profile of cells rather than an increased stress. Indeed, *DCT* is known to be expressed in human retinal progenitor cells (24) and its expression is regulated by the early RPE marker MITF. It is thus not surprising that as RPE cells mature, *MITF* expression reduces (58) and subsequently reduces *DCT* expression, as is observed in human fetal retina (24). Similarly, *CTNNB1* regulates *MITF* and *OTX2* expression and subsequently RPE differentiation (40). Finally, *SOX11* is known to be expressed in early retinal progenitor and early in differentiating RPE cells (24,48), hence its downregulation as cell culture ages further supports a maturation of RPE cells in culture. The "Young" Subpopulations Zero and One are characterised by the expression of *CST3*, which encodes for the cysteine proteinase inhibitor Cystasin. Interestingly, this protein is known to decrease in native RPE cells with aging (23). Its presence in the cell population further strengthens the suggestion of a maturing RPE population over time.

The high level of expression of mitochondrial and ribosomal -related genes in some cell populations also indicates that cells are very active, necessitating energy and ribosomal activities for protein synthesis. It could also suggest that ribosomes potentially contribute to extraribosomal functions in the RPE cells, such as cell development and maturation (19), as already reported for melanocyte development (59), retinal development (20,21) and retinal degeneration (60).

Our analysis also revealed that cells in culture can develop a transcriptomic profile more closely related to the adult native RPE. In particular one subpopulation found in both 1-month-old and 12-month-old cultures showed a profile of common RPE gene expression more closely related to the adult than to the fetal cells (27). This population could potentially be selected for assessment of more mature characteristics and phenotypes.

Conclusion

The novel insight into the underlying genetic architecture of hPSC-derived RPE cells at short and long time points in culture conditions revealed a gradual differentiation and maturation process, as well as a stable RPE phenotype over time. Most cells with a clear RPE signature are found in the "Common" subpopulation, indicating that RPE cells are present from an early time point in culture and maintain this identity with time. The clustering also reveals that whilst some subpopulations expressed more genes associated with retinal and RPE biology, other RPE subpopulations demonstrated increased expression in mitochondrial and/or ribosomal related genes. Altogether, this data suggests that hPSC-derived RPE cells develop their characteristic signature early in the differentiation process and continue to mature over time in culture. It also warrants the use of hPSC-derived RPE cells for modelling of RPE biology at early and later differentiation timings.

Materials and methods

Ethical approval

The experimental work was approved by the Human Research Ethics Committee of the University of Melbourne (1545484) with the requirements of the National Health & Medical Research Council of Australia (NHMRC) and conformed with the Declaration of Helsinki.

Cell culture and differentiation of hESCs to RPE cells

The hESC line H9 (Wicell) was maintained on vitronectin-coated plates using StemFlex (Thermo Fisher), with medium changed every second day (61). Cells were differentiated into RPE cells as previously described (3) with the following modifications. Briefly, hESCs were maintained in culture until 70-80% confluent at which stage StemFlex was replaced with Complete E6 (Stem Cell Technologies) supplemented with N2 (Thermo Fisher) to induce retinal differentiation, with thrice weekly media changes for 33 days. On Day 33, medium was replaced with RPEM (α-MEM, N1 supplement, 5% fetal bovine serum, non-essential amino acids (all Thermo Fisher), penicillin-streptomycin-glutamine (Sigma), taurine-hydrocortisone-triiodo-thyronin (THT) (in-house preparation) to promote RPE differentiation, with media changed every second day. Cells were cultured for 32 days, after which point maximal pigmentation is routinely observed. Cells were harvested with an 8-minute exposure to 0.25% Trypsin-EDTA (Thermo Fisher) and inactivated with RPEM. Non-RPE contaminants (visible as unpigmented cells), were manually removed from the culture, which begin shedding off the culture plate after ~ 2 minutes. Cells were seeded at a density of 75,000 cells / cm^2 onto growth-factor-reduced Matrigel-coated tissue culture plates (Corning). Media was changed every second day, with the first sample of cells harvested after 30 days (D30) and the second sample harvested on day 367 (D367) for scRNA-Seq analysis. (**Figure 1A**).

RPE cell harvest and single-cell preparation

RPE cells were dissociated to single cells using 0.25% Trypsin-EDTA (Thermo Fisher) for 8 min and inactivated with RPEM. Cells were centrifuged at 300g for 1 minute to pellet and resuspended in a small volume of RPEM containing 0.1% v/v propidium iodide (PI, Sigma Aldrich) to exclude non-viable cells. Single cell suspensions were passed through a 35 µm filter prior to sorting. A minimum of 60,000 live cells (PI-negative) were sorted on a BD FACSAria IIU (100 µm, 20psi) into culture medium. Cells were centrifuged at 300g for 5 min and resuspended in PBS containing 0.04% BSA to a concentration of ~800-1,000 cells/µl. Approximately 17,400 cells were loaded onto a 10X chip for a target recovery of 10,000 cells.

Generation of single cell GEMs and sequencing libraries

Single cell suspensions were loaded onto 10X Genomics Single Cell 3′ Chips along with the reverse transcription (RT) master mix as per the manufacturer's protocol for the Chromium Single Cell 3′ v2 Library (10X Genomics; PN-120233), to generate single cell gel beads in emulsion (GEMs). Sequencing libraries were generated with unique sample indices (SI) for each sample. The resulting libraries were assessed by gel electrophoresis (Agilent D1000 ScreenTape Assay) and quantified with qPCR (Illumina KAPA Library Quantification Kit). Following pooling and normalization to 4 nM, libraries were denatured and diluted to 1.6 pM for loading onto the sequencer. Libraries were sequenced on an Illumina NextSeq 500 (NextSeq Control Software v2.2.0 / Real Time Analysis v2.4.11) using NextSeq 500/550 High Output Kit v2.5 (150 Cycles) (Illumina, 20024907) as follows: 26 bp (Read 1), 8 bp (i7 Index) and 98 bp (Read 2).

Bioinformatics mapping of reads to original genes and cells

Reads underwent initial quality control, sample demultiplexing and quantification with Cell Ranger 3.0.2 by 10x Genomics (http://10xgenomics.com). Raw base calls were demultiplexed into individual samples and converted to FASTQ using the *cellranger mkfastq* pipeline. The reads were then mapped to the *Homo sapiens* genome (GRCh38, Annotation: Gencode v29) using STAR (v2.5.1b) called via the *cellranger count* pipeline. Resulting data for each sample were then aggregated and depth-equalized via the *cellranger aggr* pipeline.

Quality control and normalisation

Each sample underwent quality control independently. First, the following values were calculated for each cell: total number of Unique Molecular Identifiers (UMIs), number of detected genes and proportion of mitochondrial and ribosomal-related genes to total expression. Cells that had any of the 4 parameter measurements lower than 3x median absolute deviation (MAD) of all cells were removed from subsequent analysis. Cells were also removed if mitochondrial-associated genes accounted for more than 25% of total expression, and/or ribosomal-associated genes accounted for more than 60% of total expression. Cell-cell normalization was then performed using the SCTransform function from Seurat (62). Confounding sources of variation - specifically, mitochondrial and ribosomal mapping percentage, were also regressed out with this function.

Dimensionality reduction, clustering and integration

The dimensionality of the data was first reduced with Principal Component Analysis (PCA). Subsequently, the 30 most statistically significant principal components (PCs) were reduced to two dimensions by Uniform Manifold Approximation Projection (UMAP). These values were used to construct a Shared Nearest Neighbour (SNN) graph for each cell. The Louvain method

for community detection was then used to identify clusters in each dataset at the resolution of 0.6. The 1-month and 12-month datasets were then integrated using Seurat's SCTransform integration method (16). The unsupervised version of MetaNeighbor was used to evaluate the similarities between the 1-month clusters and 12-month clusters. Cluster pairs that received an Area Under the Receiver Operating Characteristic (AUROC) score greater than 0.9 were merged into one cluster (**Supplementary Figure 2**).

Clustering characterization and analysis

Network analysis was then performed on significant differentially-expressed genes using Reactome functional interaction analysis (63,64). Gene Ontology (GO) analysis was performed using (13,14).

Code availability

All code and usage notes are available at: https://github.com/powellgenomicslab/RPE_scRNA_AgedStudy. This repository consists of code used to process raw sequencing data in FASTQ format to cell-gene expression tables via the Cell Ranger pipeline, and code used to perform the following analysis: quality control, normalization, dimensionality reduction, clustering, differential expression and integration.

Data Records

Data is available at ArrayExpress (accession number E-MTAB-851). Files consist of raw FASTQ files, and a tab separated matrix of UMIs per gene for each cell passing quality control filtering. BAM files can be generated by using the supplied repository to process the FASTQ files via Cell Ranger.

Authors' contributions

Category 1, Conception and design of study; acquisition of data analysis and/or interpretation of data: GEL, AS, CA, VG, DCK, DAZ, ELF, SHN, AWH, JP, AP.

Category 2, Drafting the manuscript; revising the manuscript critically for important intellectual content: GEL, AS, JP, AP.

Category 3, Approval of the version of the manuscript to be published: GEL, AS, CA, VG, DCK, DAZ, ELF, SHN, AWH, JP, AP.

Competing interests

The authors have declared no competing interests.

References

1. Perez VL, Saeed AM, Tan Y, Urbieta M, Cruz-Guilloty F. The eye: A window to the soul of the immune system. J Autoimmun. 2013 Sep;45:7–14.

2. Xu H, Chen M, Forrester JV. Para-inflammation in the aging retina. Prog Retin Eye Res. 2009 Sep;28(5):348–68.

3. Lidgerwood GE, Morris AJ, Conquest A, Daniszewski M, Rooney LA, Lim SY, et al. Role of lysophosphatidic acid in the retinal pigment epithelium and photoreceptors. Biochim Biophys Acta Mol Cell Biol Lipids. 2018 Jul;1863(7):750–61.

4. Lidgerwood GE, Lim SY, Crombie DE, Ali R, Gill KP, Hernández D, et al. Defined

Medium Conditions for the Induction and Expansion of Human Pluripotent Stem Cell-Derived Retinal Pigment Epithelium. Stem Cell Rev. 2016 Apr;12(2):179–88.

5. Kamao H, Mandai M, Okamoto S, Sakai N, Suga A, Sugita S, et al. Characterization of Human Induced Pluripotent Stem Cell-Derived Retinal Pigment Epithelium Cell Sheets Aiming for Clinical Application [Internet]. Vol. 2, Stem Cell Reports. 2014. p. 205–18. Available from: http://dx.doi.org/10.1016/j.stemcr.2013.12.007

6. Skottman H, Vaajasaari H, Nymark S, Juuti-Uusitalo K, Hyttinen J, Uusitalo H, et al. Human pluripotent stem cell derived retinal pigment epithelium fulfills requirements of the in vitro functionality [Internet]. Vol. 90, Acta Ophthalmologica. 2012. p. 0–0. Available from: http://dx.doi.org/10.1111/j.1755-3768.2012.4484.x

7. Osakada F, Jin Z-B, Hirami Y, Ikeda H, Danjyo T, Watanabe K, et al. In vitro differentiation of retinal cells from human pluripotent stem cells by small-molecule induction. J Cell Sci. 2009 Sep 1;122(Pt 17):3169–79.

8. Klimanskaya I. Retinal Pigment Epithelium Derived from Embryonic Stem Cells [Internet]. Principles of Regenerative Medicine. 2008. p. 852–66. Available from: http://dx.doi.org/10.1016/b978-012369410-2.50051-6

9. Buchholz DE, Pennington BO, Croze RH, Hinman CR, Coffey PJ, Clegg DO. Rapid and efficient directed differentiation of human pluripotent stem cells into retinal pigmented epithelium. Stem Cells Transl Med. 2013 May;2(5):384–93.

10. Foltz LP, Clegg DO. Rapid, Directed Differentiation of Retinal Pigment Epithelial Cells from Human Embryonic or Induced Pluripotent Stem Cells [Internet]. Journal of Visualized

Experiments. 2017. Available from: http://dx.doi.org/10.3791/56274

11. Bennis A, Jacobs JG, Catsburg LAE, ten Brink JB, Koster C, Schlingemann RO, et al. Stem Cell Derived Retinal Pigment Epithelium: The Role of Pigmentation as Maturation Marker and Gene Expression Profile Comparison with Human Endogenous Retinal Pigment Epithelium [Internet]. Vol. 13, Stem Cell Reviews and Reports. 2017. p. 659–69. Available from: http://dx.doi.org/10.1007/s12015-017-9754-0

12. Kokkinaki M, Sahibzada N, Golestaneh N. Human Induced Pluripotent Stem-Derived Retinal Pigment Epithelium (RPE) Cells Exhibit Ion Transport, Membrane Potential, Polarized Vascular Endothelial Growth Factor Secretion, and Gene Expression Pattern Similar to Native RPE [Internet]. Vol. 29, STEM CELLS. 2011. p. 825–35. Available from: http://dx.doi.org/10.1002/stem.635

13. Ashburner M, Ball CA, Blake JA, Botstein D, Butler H, Cherry JM, et al. Gene ontology: tool for the unification of biology. The Gene Ontology Consortium. Nat Genet. 2000 May;25(1):25–9.

14. The Gene Ontology Consortium, The Gene Ontology Consortium. The Gene Ontology Resource: 20 years and still GOing strong [Internet]. Vol. 47, Nucleic Acids Research. 2019. p. D330–8. Available from: http://dx.doi.org/10.1093/nar/gky1055

15. McDavid A, Finak G, Chattopadyay PK, Dominguez M, Lamoreaux L, Ma SS, et al. Data exploration, quality control and testing in single-cell qPCR-based gene expression experiments. Bioinformatics. 2013 Feb 15;29(4):461–7.

16. Stuart T, Butler A, Hoffman P, Hafemeister C, Papalexi E, Mauck WM 3rd, et al.

Comprehensive Integration of Single-Cell Data. Cell. 2019 Jun 13;177(7):1888–902.e21.

17. Crow M, Paul A, Ballouz S, Huang ZJ, Gillis J. Characterizing the replicability of cell types defined by single cell RNA-sequencing data using MetaNeighbor. Nat Commun. 2018 Feb 28;9(1):884.

18. Tarau I-S, Berlin A, Curcio CA, Ach T. The Cytoskeleton of the Retinal Pigment Epithelium: from Normal Aging to Age-Related Macular Degeneration. Int J Mol Sci [Internet]. 2019 Jul 22;20(14). Available from: http://dx.doi.org/10.3390/ijms20143578

19. Zhou X, Liao W-J, Liao J-M, Liao P, Lu H. Ribosomal proteins: functions beyond the ribosome. J Mol Cell Biol. 2015 Apr;7(2):92.

20. Barkić M, Crnomarković S, Grabusić K, Bogetić I, Panić L, Tamarut S, et al. The p53 tumor suppressor causes congenital malformations in Rpl24-deficient mice and promotes their survival. Mol Cell Biol. 2009 May;29(10):2489–504.

21. Watkins-Chow DE, Cooke J, Pidsley R, Edwards A, Slotkin R, Leeds KE, et al. Mutation of the diamond-blackfan anemia gene Rps7 in mouse results in morphological and neuroanatomical phenotypes. PLoS Genet. 2013 Jan 31;9(1):e1003094.

22. Paraoan L, Grierson I, Maden BE. Analysis of expressed sequence tags of retinal pigment epithelium: cystatin C is an abundant transcript. Int J Biochem Cell Biol. 2000 Apr;32(4):417–26.

23. Kay P, Yang YC, Hiscott P, Gray D, Maminishkis A, Paraoan L. Age-related changes of cystatin C expression and polarized secretion by retinal pigment epithelium: potential age-

related macular degeneration links. Invest Ophthalmol Vis Sci. 2014 Feb 14;55(2):926–34.

24. Hu Y, Wang X, Hu B, Mao Y, Chen Y, Yan L, et al. Dissecting the transcriptome landscape of the human fetal neural retina and retinal pigment epithelium by single-cell RNA-seq analysis. PLoS Biol. 2019 Jul;17(7):e3000365.

25. Guyonneau L, Murisier F, Rossier A, Moulin A, Beermann F. Melanocytes and pigmentation are affected in dopachrome tautomerase knockout mice. Mol Cell Biol. 2004 Apr;24(8):3396–403.

26. Takeda K, Yokoyama S, Yasumoto K-I, Saito H, Udono T, Takahashi K, et al. OTX2 regulates expression of DOPAchrome tautomerase in human retinal pigment epithelium. Biochem Biophys Res Commun. 2003 Jan;300(4):908–14.

27. Strunnikova NV, Maminishkis A, Barb JJ, Wang F, Zhi C, Sergeev Y, et al. Transcriptome analysis and molecular signature of human retinal pigment epithelium. Hum Mol Genet. 2010 Jun 15;19(12):2468–86.

28. Strunnikova N, Zhang C, Teichberg D, Cousins SW, Baffi J, Becker KG, et al. Survival of retinal pigment epithelium after exposure to prolonged oxidative injury: a detailed gene expression and cellular analysis. Invest Ophthalmol Vis Sci. 2004 Oct;45(10):3767–77.

29. Tanaka Y, Utsumi J, Matsui M, Sudo T, Nakamura N, Mutoh M, et al. Purification, molecular cloning, and expression of a novel growth-promoting factor for retinal pigment epithelial cells, REF-1/TFPI-2. Invest Ophthalmol Vis Sci. 2004 Jan;45(1):245–52.

30. Alizadeh P, Smit-McBride Z, Oltjen SL, Hjelmeland LM. Regulation of cysteine cathepsin

expression by oxidative stress in the retinal pigment epithelium/choroid of the mouse. Exp Eye Res. 2006 Sep;83(3):679–87.

31. Samuel W, Kutty RK, Vijayasarathy C, Pascual I, Duncan T, Redmond TM. Decreased expression of insulin-like growth factor binding protein-5 during N-(4-hydroxyphenyl)retinamide-induced neuronal differentiation of ARPE-19 human retinal pigment epithelial cells: regulation by CCAAT/enhancer-binding protein. J Cell Physiol. 2010 Sep;224(3):827–36.

32. Quinn PM, Buck TM, Mulder AA, Ohonin C, Alves CH, Vos RM, et al. Human iPSC-Derived Retinas Recapitulate the Fetal CRB1 CRB2 Complex Formation and Demonstrate that Photoreceptors and Müller Glia Are Targets of AAV5. Stem Cell Reports. 2019 May 14;12(5):906–19.

33. Paniagua AE, Herranz-Martín S, Jimeno D, Jimeno ÁM, López-Benito S, Carlos Arévalo J, et al. CRB2 completes a fully expressed Crumbs complex in the Retinal Pigment Epithelium. Sci Rep. 2015 Sep 25;5:14504.

34. Winokur PN, Subramanian P, Bullock JL, Arocas V, Becerra SP. Comparison of two neurotrophic serpins reveals a small fragment with cell survival activity. Mol Vis. 2017 Jul 3;23:372–84.

35. Chang JT, Esumi N, Moore K, Li Y, Zhang S, Chew C, et al. Cloning and characterization of a secreted frizzled-related protein that is expressed by the retinal pigment epithelium. Hum Mol Genet. 1999 Apr;8(4):575–83.

36. Liu NP, Roberts WL, Hale LP, Levesque MC, Patel DD, Lu CL, et al. Expression of CD44

and variant isoforms in cultured human retinal pigment epithelial cells. Invest Ophthalmol Vis Sci. 1997 Sep;38(10):2027–37.

37. Uhlén M, Fagerberg L, Hallström BM, Lindskog C, Oksvold P, Mardinoglu A, et al. Proteomics. Tissue-based map of the human proteome. Science. 2015 Jan 23;347(6220):1260419.

38. Bennis A, Ten Brink JB, Moerland PD, Heine VM, Bergen AA. Comparative gene expression study and pathway analysis of the human iris- and the retinal pigment epithelium. PLoS One. 2017 Aug 21;12(8):e0182983.

39. Cao L, Liu J, Pu J, Milne G, Chen M, Xu H, et al. Polarized retinal pigment epithelium generates electrical signals that diminish with age and regulate retinal pathology. J Cell Mol Med. 2018 Nov;22(11):5552–64.

40. Westenskow P, Piccolo S, Fuhrmann S. Beta-catenin controls differentiation of the retinal pigment epithelium in the mouse optic cup by regulating Mitf and Otx2 expression. Development. 2009 Aug;136(15):2505–10.

41. Lee W-H, Joshi P, Wen R. Glutathione S-transferase pi isoform (GSTP1) expression in murine retina increases with developmental maturity. Adv Exp Med Biol. 2014;801:23–30.

42. Wang AL, Lukas TJ, Yuan M, Du N, Tso MO, Neufeld AH. Autophagy and exosomes in the aged retinal pigment epithelium: possible relevance to drusen formation and age-related macular degeneration. PLoS One. 2009 Jan 8;4(1):e4160.

43. Pasovic L, Utheim TP, Reppe S, Khan AZ, Jackson CJ, Thiede B, et al. Improvement of

Storage Medium for Cultured Human Retinal Pigment Epithelial Cells Using Factorial Design. Sci Rep. 2018 Apr 9;8(1):5688.

44. Cai H, Shin MC, Tezel TH, Kaplan HJ, Del Priore LV. Use of iris pigment epithelium to replace retinal pigment epithelium in age-related macular degeneration: a gene expression analysis. Arch Ophthalmol. 2006 Sep;124(9):1276–85.

45. Alge CS, Suppmann S, Priglinger SG, Neubauer AS, May CA, Hauck S, et al. Comparative proteome analysis of native differentiated and cultured dedifferentiated human RPE cells. Invest Ophthalmol Vis Sci. 2003 Aug;44(8):3629–41.

46. Wang D, Chadha GK, Feygin A, Ivanov AI. F-actin binding protein, anillin, regulates integrity of intercellular junctions in human epithelial cells. Cell Mol Life Sci. 2015 Aug;72(16):3185–200.

47. Li Y, Hao H, Tzatzalos E, Lin R-K, Doh S, Liu LF, et al. Topoisomerase IIbeta is required for proper retinal development and survival of postmitotic cells. Biol Open. 2014 Feb 15;3(2):172–84.

48. Usui A, Mochizuki Y, Iida A, Miyauchi E, Satoh S, Sock E, et al. The early retinal progenitor-expressed gene Sox11 regulates the timing of the differentiation of retinal cells. Development. 2013 Feb;140(4):740–50.

49. van Soest SS, de Wit GMJ, Essing AHW, ten Brink JB, Kamphuis W, de Jong PTVM, et al. Comparison of human retinal pigment epithelium gene expression in macula and periphery highlights potential topographic differences in Bruch's membrane. Mol Vis. 2007 Sep 10;13:1608–17.

50. Tian J, Ishibashi K, Honda S, Boylan SA, Hjelmeland LM, Handa JT. The expression of native and cultured human retinal pigment epithelial cells grown in different culture conditions. Br J Ophthalmol. 2005 Nov;89(11):1510–7.

51. Whitmore SS, Wagner AH, DeLuca AP, Drack AV, Stone EM, Tucker BA, et al. Transcriptomic analysis across nasal, temporal, and macular regions of human neural retina and RPE/choroid by RNA-Seq. Exp Eye Res. 2014 Dec;129:93–106.

52. Cai H, Fields MA, Hoshino R, Priore LVD. Effects of aging and anatomic location on gene expression in human retina. Front Aging Neurosci. 2012 May 31;4:8.

53. Toomey CB, Johnson LV, Bowes Rickman C. Complement factor H in AMD: Bridging genetic associations and pathobiology. Prog Retin Eye Res. 2018 Jan;62:38–57.

54. Yang P, Skiba NP, Tewkesbury GM, Treboschi VM, Baciu P, Jaffe GJ. Complement-Mediated Regulation of Apolipoprotein E in Cultured Human RPE Cells. Invest Ophthalmol Vis Sci. 2017 Jun 1;58(7):3073–85.

55. Liao J-L, Yu J, Huang K, Hu J, Diemer T, Ma Z, et al. Molecular signature of primary retinal pigment epithelium and stem-cell-derived RPE cells. Hum Mol Genet. 2010 Nov 1;19(21):4229–38.

56. May-Simera HL, Wan Q, Jha BS, Hartford J, Khristov V, Dejene R, et al. Primary Cilium-Mediated Retinal Pigment Epithelium Maturation Is Disrupted in Ciliopathy Patient Cells. Cell Rep. 2018 Jan 2;22(1):189–205.

57. Rodríguez-Menéndez S, García M, Fernández B, Álvarez L, Fernández-Vega-Cueto A,

Coca-Prados M, et al. The Zinc-Metallothionein Redox System Reduces Oxidative Stress in Retinal Pigment Epithelial Cells. Nutrients [Internet]. 2018 Dec 2;10(12). Available from: http://dx.doi.org/10.3390/nu10121874

58. Capowski EE, Simonett JM, Clark EM, Wright LS, Howden SE, Wallace KA, et al. Loss of MITF expression during human embryonic stem cell differentiation disrupts retinal pigment epithelium development and optic vesicle cell proliferation. Hum Mol Genet. 2014 Dec 1;23(23):6332–44.

59. McGowan KA, Li JZ, Park CY, Beaudry V, Tabor HK, Sabnis AJ, et al. Ribosomal mutations cause p53-mediated dark skin and pleiotropic effects. Nat Genet. 2008 Aug;40(8):963–70.

60. Grewal R, Stepczynski J, Kelln R, Erickson T, Darrow R, Barsalou L, et al. Coordinated changes in classes of ribosomal protein gene expression is associated with light-induced retinal degeneration. Invest Ophthalmol Vis Sci. 2004 Nov;45(11):3885–95.

61. Daniszewski M, Nguyen Q, Chy HS, Singh V, Crombie DE, Kulkarni T, et al. Single-Cell Profiling Identifies Key Pathways Expressed by iPSCs Cultured in Different Commercial Media. iScience. 2018 Sep 28;7:30–9.

62. Hafemeister C, Satija R. Normalization and variance stabilization of single-cell RNA-seq data using regularized negative binomial regression. Genomics. bioRxiv; 2019. p. 861.

63. Anders S, Huber W. Differential expression analysis for sequence count data [Internet]. Nature Precedings. 2010. Available from: http://dx.doi.org/10.1038/npre.2010.4282.2

64. Wu G, Feng X, Stein L. A human functional protein interaction network and its application to cancer data analysis. Genome Biol. 2010 May 19;11(5):R53.

Figure Legends

Figure 1: scRNA-seq transcriptome profiling of hPSC-derived RPE cells. (**A**) Schematic representations of the experimental flow and (**B**) of cluster grouping, showing Young, Aged and their common subpopulations with associated Table. (**C**) Uniform Manifold Approximation and Projection for Dimension Reduction (UMAP) of single cell- expression profile from 16,576 cells, clustering into 18 subpopulations, and split by condition (1-month- and 12-month-old). (**D**) Dot plot of canonical RPE markers in all subpopulations. Population arising from 1-month-old cultures are represented in blue and those from 12-month-old cultures in red. Subpopulations are indicated by numbers. Size of the dot indicates levels of expression per subpopulation.

Figure 2: scRNA-seq transcriptome profiling of hPSC-derived RPE cells. Heatmap showing the top 10 most conserved markers (gene transcripts are indicated on the left side) in all individual cells of each 18 subpopulation (indicated on top, with color matching subpopulations of Figure 1C). The intensity of gene expression is indicated by colour variation.

Figure 3: Expression patterns of selected conserved markers in RPE in the hPSC-derived RPE cells. (**A**) UMAP of single cell- expression profile from 12-month-old ("Aged") and 1-month-old ("Control") cells for selected identified cluster markers. Levels of gene expression are shown with colour gradients. Violin plots of selected conserved markers in each "Common" subpopulation characteristic of neural differentiation **(B)**; extracellular matrix **(C)** and the RPE **(D)**. The plots describe the distribution and relative expression of each transcript in each subpopulation, with separation of cells belonging to the 1-month-old ("Control") and 12-month-old ("Aged") cultures.

Figure 4: Selected gene ontology pathway analysis. (**A**) GO pathways associated with each of the "Common" subpopulations (1-6), with fold enrichment per subpopulation. **(B)** UMAP of single cell- expression profile with renamed clusters representing "Young", "Common" and "Aged" subpopulations. (**C**) Examples of genes from selected pathways represented by violin plots in the three subpopulations ("Young", "Aged", "Common", represented in different colours). The plots describe the distribution and relative expression of each transcript in the three main subpopulations.

Figure 5: Expression patterns of representative markers of mature native RPE in the hPSC-derived RPE cells. (**A**) Violin plots of selected markers representative of mature native RPE cells (obtained from (27) in the three subpopulations ("Young", "Aged", "Common", represented in different colours). The plots describe the distribution and relative expression of each transcript in the three main subpopulations. **(B)** Ridge plots and **(C)** feature plots of expression profiles of key metallothioneins across all subpopulations, and across the two conditions ("Young" and "Aged").

Supplementary Figure Legends

Supplementary Figure 1: Filtering of cells based on quality control with proportion of reads mapped to mitochondrial- and ribosomal- related transcripts. (**A**) Total Unique molecular identifiers (UMIs) per cell, UMI threshold manually set to 100-30,000. (**B**) Total gene per cell, threshold manually set to 220. (**C**) Mitochondrial and ribosomal -related gene expression (in %). Thresholds for mitochondrial count set at 25% and for ribosomal expression at 60%. (**D**) PCA plot of the scaled data. 1: 1-month-old cells; 2: 12-month-old cells.

Supplementary Figure 2: Clustering resolution. Clustering resolution of (**A**) 1-month-old cells, (**B**) 12-month-old cells and (**C**) integrated (combined) datasets.

Supplementary Tables

Supplementary Table 1. Quality control parameters.

Supplementary Table 2. Cluster analysis with number of cells per subpopulation.

Supplementary Table 3. Conserved cluster markers, GO pathways and differential expression for each subpopulation within the "Common" Subpopulations. Cluster (pct.1) shows frequency of cells expressing a marker compared to all others (pct.2). avg_logFC: average level of expression per cell in subpopulations compared to all others.

Supplementary Table 4. Conserved cluster markers and GO pathways for each subpopulation within the "Young" Subpopulations. Cluster (pct.1) shows frequency of cells expressing a marker compared to all others (pct.2). avg_logFC: average level of expression per cell in subpopulations compared to all others.

Supplementary Table 5. Conserved cluster markers and GO pathways for each subpopulation within the "Aged" Subpopulations. Cluster (pct.1) shows frequency of cells expressing a marker compared to all others (pct.2). avg_logFC: average level of expression per cell in subpopulations compared to all others.

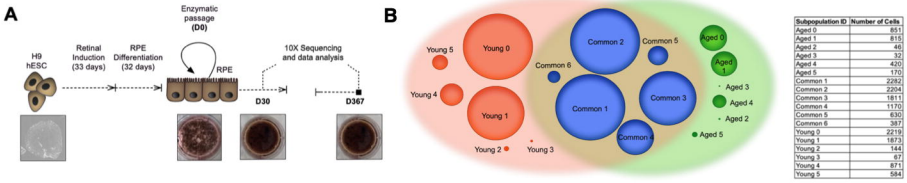

Subpopulation ID	Number of Cells
Aged 0	851
Aged 1	815
Aged 2	46
Aged 3	32
Aged 4	420
Aged 5	170
Common 1	2282
Common 2	2204
Common 3	1811
Common 4	1170
Common 5	630
Common 6	387
Young 0	2219
Young 1	1873
Young 2	144
Young 3	67
Young 4	871
Young 5	584